Published in final edited form as:
J Org Chem. 2013 October 4; 78(19): . doi:10.1021/jo4015936.

Identification and characterization of 2nd generation Invader Locked Nucleic Acids (LNAs) for mixed-sequence recognition of double-stranded DNA

Sujay P. Sau[a], **Andreas S. Madsen**[b], **Peter Podbevsek**[c], **Nicolai K. Andersen**[b], **T. Santhosh Kumar**[b], **Sanne Andersen**[a,b], **Rie L. Rathje**[a,b], **Brooke A. Anderson**[a], **Dale C. Guenther**[a], **Saswata Karmakar**[a], **Pawan Kumar**[a], **Janez Plavec**[c], **Jesper Wengel**[b], and **Patrick J. Hrdlicka**[a]

Patrick J. Hrdlicka: hrdlicka@uidaho.edu

[a]Department of Chemistry, University of Idaho, Moscow, ID-83844, USA

[b]Nucleic Acid Center, Department of Physics and Chemistry, University of Southern Denmark, Odense, Denmark

[c]National Institute of Chemistry, Ljubljana, Slovenia

Abstract

Development of synthetic agents that recognize double-stranded DNA (dsDNA) is a long-standing goal that is inspired by the promise for tools that detect, regulate and modify genes. Progress has been made with triplex-forming oligonucleotides, PNAs, and polyamides, but substantial efforts are currently devoted to the development of alternative strategies that overcome limitations observed with the classic approaches. In 2005, we introduced Invader Locked Nucleic Acids (LNAs), i.e., double-stranded probes that are activated for mixed-sequence recognition of dsDNA through modification with '+1 interstrand zippers' of 2'-*N*-(pyren-1-yl)methyl-2'-amino-α-L-LNA monomers. Despite promising preliminary results, progress has been slow due to the synthetic complexity of the building blocks. Here, we describe a study that led to the identification of two simpler classes of Invader monomers. We compare thermal denaturation characteristics of double-stranded probes featuring different interstrand zippers of pyrene-functionalized monomers based on 2'-amino-α-L-LNA, 2'-*N*-methyl-2'-amino-DNA, and RNA scaffolds. Insights from fluorescence spectroscopy, molecular modeling and NMR spectroscopy are used to elucidate the structural factors that govern probe activation. We demonstrate that probes with +1 zippers of 2'-*O*-(pyren-1-yl)methyl-RNA or 2'-*N*-methyl-2'-*N*-(pyren-1-yl)methyl-2'-amino-DNA monomers recognize DNA hairpins with similar efficiency as original Invader LNAs. Access to synthetically simple monomers will accelerate the use of Invader-mediated dsDNA-recognition for applications in molecular biology and nucleic acid diagnostics.

Introduction

Development of strategies for sequence-unrestricted targeting of double-stranded DNA (dsDNA) continues to be one of the great challenges of biological chemistry. Efforts are fuelled by the promise for powerful molecular tools that enable gene regulation, modification and detection, and for drug candidates against genetic diseases.[1-6] Significant

Correspondence to: Patrick J. Hrdlicka, hrdlicka@uidaho.edu.

Supporting information: MS-data for **R**-modified ONs; thermal denaturation properties of double-stranded probes with 'mixed' zippers; lowest energy structure of **W2:W5;** NOESY spectrum of **W13a:W13b;** dose-response curves and additional gel electropherograms. This material is available free of charge via the Internet at http://pubs.acs.org/.

progress toward this end was originally made with triplex-forming oligonucleotides (TFOs), peptide nucleic acids (PNAs), and minor-groove binding polyamides.[7-11] However, these classic dsDNA-targeting approaches display limitations, which has restricted their widespread use. For example, TFOs and regular PNAs only recognize homopurine targets, most PNA-based approaches require non-physiological salinity, and polyamides are typically only used against short target regions, which precludes recognition of unique targets in the genome. These drawbacks have spurred development of alternative strategies for mixed-sequence recognition of dsDNA such as pseudocomplementary (pc) DNA,[12] pcPNA,[13,14] antigene PNA,[15] antigene locked nucleic acid (LNA),[16] γ-PNA,[17,18] TFOs with engineered nucleobases,[19,20] engineered proteins,[21,22] and other approaches.[23-28] Nonetheless, there remains a need for probes that enable rapid, potent and specific targeting of mixed-sequence dsDNA at physiologically relevant conditions, and which are inexpensive, compatible with delivery agents, and amenable for large scale production.

In 2005, we introduced Invader LNAs as an alternative strategy for mixed-sequence dsDNA-recognition.[29] Briefly described, Invader LNAs are double-stranded probes, which are activated for dsDNA-recognition through modification with one or more '+1 interstrand zippers' of 2'-*N*-(pyren-1-yl)methyl-2'-amino-α-L-LNA **W** monomers (Figs. 1 and 2; for a definition of the zipper nomenclature, see reference 30). This particular monomer arrangement results in duplex destabilization, presumably since the pyrene moieties are forced to intercalate into the same region, leading to excessive local duplex unwinding and formation of 'energetic hotspots' (Fig. 1).[29,31] On the other hand, the two strands that comprise an Invader LNA, display very strong affinity toward complementary single-stranded DNA (ssDNA) due to efficient pyrene intercalation and π-π-stacking with neighboring base pairs (Fig. 1).[29,31,32] We have used the difference in thermostability between Invader LNAs and probe-target duplexes to realize mixed-sequence recognition of short iso-sequential dsDNA targets (Fig. 1).[29,31] For example, addition of a 13-mer Invader LNA with two energetic hotspots to equimolar quantities of an iso-sequential dsDNA target, results in ~50% recognition within ~30 min (110 mM NaCl, pH 7, T_{exp} = 20 °C).[31] The recognition likely entails partial unwinding of probe and/or target duplexes, but does not appear to require full duplex dissociation.

A related dsDNA-targeting approach, in which DNA duplexes with adjacent incorporations of intercalator-modified non-nucleotide monomers were used to inhibit in vitro transcription in cell-free assays, appeared in the scientific literature[26] following our original studies.[29] NMR studies have shown that this approach relies on intercalator-mediated duplex unwinding for probe destabilization,[33] in a similar manner as hypothesized for Invader LNAs.

In spite of the interesting initial results, progress with Invader LNAs has been slow, in large part due to the difficult synthesis of the corresponding phosphoramidite of monomer **W** (~3% yield from diacetone-α-D-glucose over ~20 steps).[32] A promise for synthetically more readily accessible Invader building blocks came when we discovered that oligodeoxyribonucleotides (ONs) modified with 2'-*O*-(pyren-1-yl)methyluridine monomer **P** or 2'-*N*-methyl-2'-*N*-(pyren-1-yl)methyl-2'-aminodeoxyuridine monomer **Q** (Fig. 2), display similar affinity toward complementary DNA as **W**-modified ONs,[34] since their pyrene moieties also are predisposed for intercalation into DNA duplexes.[34-36] Importantly, the corresponding phosphoramidites are obtained from uridine in only four and seven steps, respectively.[34] Indeed, we have recently demonstrated that monomer **P** can be used *in lieu* of the original LNA-based building block **W** to generate second-generation Invaders that recognize chromosomal DNA in non-denaturing FISH experiments, marking a proof-of-concept for Invader-mediated mixed-sequence recognition of biological dsDNA.[37]

In the present article, we describe the process that resulted in the identification of the second-generation Invader building blocks **Q, P** and **R**. At the onset of this study, we had the following goals: i) examine if the thermal activation observed for double-stranded probes with +1 interstrand zippers of 2'-*N*-(pyren-1-yl)methyl-2'-amino-α-L-LNA T monomers is a unique property of **W** monomers, or if it can be emulated or even optimized using other zipper arrangements and/or building blocks (Fig. 2); ii) determine the structural factors that govern thermal activation of duplexes with certain interstrand zipper arrangements of pyrene-functionalized nucleotides; and iii) demonstrate Invader-mediated mixed-sequence recognition of challenging dsDNA targets.

Results and Discussion

Synthesis of ONs

For the present study we utilized a series of singly modified 9-mer ONs, the vast majority of which have been prepared and characterized with respect to identity (MALDI-MS) and purity (>80%, ion-pair reverse-phase HPLC) in previous studies.[32,34,38,39] Synthesis and characterization of new ONs (**P3** and **R**-series) is described in the supporting information. ONs containing a single modification in the 5'-G**B**G ATA TGC context are denoted **N1, O1, P1**, etc. Similar conventions apply for ONs in the **B2**-**B9** series (Tables 1 and 2).

Hybridization characteristics of pyrene-functionalized ONs with ssDNA targets

We have previously demonstrated that 9-mer ONs, which are singly modified with N2'-pyrene-functionalized 2'-amino-α-L-LNA thymine monomers **W**-**Z** (Fig. 2), display greatly increased thermal affinity toward ssDNA relative to unmodified ONs (ΔT_m between +0.5 and +19.5 °C, Table 1).[32] The degree of duplex stabilization depends on the strength of the stacking interactions between the intercalating pyrene and the flanking nucleobases. This, concomitantly, depends on the specific nature of the 3'-flanking nucleotide (purines induce greater stabilization than pyrimidines) and the linker between the pyrene moiety and the bicyclic sugar skeleton. Monomers with short linkers result in greater duplex stabilization than monomers with long linkers (trend: **X**>**Y**≫**Z**). Moreover, monomers in which the pyrene is attached via an acyl linker induce greater stabilization than monomers using alkyl linkers (trend: **X**>**W**). Similar trends are observed for ONs modified with the corresponding adenine monomers **K/L/M** (Fig. 2 and Table 2).[39] In contrast, ONs that are singly modified with 2'-oxy-α-L-LNA thymine monomer **O** or non-functionalized 2'-amino-α-L-LNA thymine monomer **N** display more moderate affinity toward ssDNA (Fig. 2 and Table 1),[32] which underscores the important stabilizing role of the pyrenes of monomers **W**-**Z**.

We have recently demonstrated that ONs modified with N2'-pyrene-functionalized 2'-*N*-methyl-2'-aminodeoxyuridine monomers **Q/S/V** display highly linker-dependent variations in ssDNA affinity (Fig. 2). With this compound class, alkyl linkers induce far greater ssDNA affinity than monomers with acyl linkers (ΔT_m values vary from -6.0 to +14.0 °C, trend: **Q**≫**V**>**S**, Table 1).[34] Importantly, ONs modified with 2'-*N*-methyl-2'-*N*-(pyren-1-yl)methyl-2'-aminodeoxyuridine monomer **Q** - or the closely related 2'-*O*-(pyren-1-yl)methyluridine monomer **P** - display similar ssDNA affinity as ONs modified with the original Invader building block **W** (Table 1).[34] An equivalent relationship is observed for ONs modified with adenine monomers **R** and **K** (Fig. 2 and Table 2), supporting our hypothesis that certain N2'-pyrene-functionalized 2'-*N*-methyl-2'-amino-DNA and O2'-pyrene-functionalized-RNA monomers are mimics of synthetically more elaborate N2'-pyrene-functionalized 2'-amino-α-L-LNA monomers.

Thermostability of duplexes with interstrand arrangements of pyrene-functionalized monomers

The thermostability of DNA duplexes with different interstrand zipper arrangements of pyrene-functionalized monomers was measured to identify monomers and probe architectures that are activated for dsDNA-recognition via the Invader strategy (Table 3). The impact on duplex stability upon incorporation of a second monomer can be additive, cooperative (i.e., more-than-additive) or antagonistic (i.e., less-than-additive) relative to a corresponding singly modified duplex. This is readily estimated by the term '*deviation from additivity*' (*DA*) defined as: $DA_{\mathbf{ONX:ONY}} \equiv \Delta T_m$ (**ONX:ONY**) − [ΔT_m (**ONX**:ssDNA) + ΔT_m (ssDNA:**ONY**)] where **ONX:ONY** is a duplex with an interstrand monomer arrangement. Double-stranded probes with highly negative *DA* values are thermally activated for recognition of iso-sequential dsDNA via the process depicted in Figure 1, as this indicates that the probe-target duplexes are more thermostable than the Invader probe and dsDNA target.

As previously reported,[29] duplexes with +4 or -3 interstrand zippers of **W** monomers, are i) strongly stabilized relative to unmodified DNA duplexes due to additive contributions from both monomers and ii) not activated for dsDNA-recognition (i.e., ΔT_m's $\gg$ 0 °C and *DA* ~ 0 °C, Table 3). While rather stable, duplexes with -1 interstrand zippers of **W** monomers display less-than-additive increases in thermostability and are weakly activated for dsDNA-recognition (i.e., ΔT_m's $\gg$ 0 °C and *DA* < 0 °C, Table 3). Duplexes with +2, and in particular, +1 zippers are far more destabilized and strongly activated (i.e., ΔT_m's ~ 0 °C and *DA* $\ll$ 0 °C, Table 3). As previously mentioned, +1 zippers of **W** monomers are the structural elements that were used to realize Invader-mediated recognition of iso-sequential dsDNA targets in our original studies.[29,31]

In contrast, control duplexes with two conventional 2'-oxy-α-L-LNA thymine monomers are highly thermostable, regardless of the relative monomer arrangement, due to additive contributions from both monomers (i.e., ΔT_m's $\gg$ 0 °C and *DA* ~ 0 °C, data for **O** monomers, Table 3). Duplexes with two 2'-amino-α-L-LNA thymine **N** monomers in +4/+2/-3 arrangements are not thermally activated for dsDNA-recognition, while duplexes with +1/-1 zippers are mildly activated (*DA* between -8.5 and -4.0 °C, Table 3). We speculate that the latter is a result of electrostatic repulsion between two proximal and partially protonated 2'-amino-α-L-LNA monomers. These control experiments demonstrate that the pyrenes of the two **W** monomers play a key role in activating +1 zipper probe **W2:W5**, whereas the presence of two proximal α-L-LNA skeletons is less important. This suggested to us that non-LNA-based monomers could be used to activate double-stranded probes for dsDNA-recognition via the approach depicted in Figure 1.

The hybridization characteristics of duplexes with interstrand arrangements of two 2'-*N*-(pyren-1-yl)carbonyl-2'-amino-α-L-LNA thymine **X** monomers resemble those of the corresponding **W**-series (Table 3), i.e., roughly additive contributions in thermostability with +4 and -3 zippers, mildly antagonistic effects with -1 zippers, and strong activation with +2 and +1 zippers. Interestingly, +1 zipper duplex **X2:X5** is more strongly activated than **W2:W5** ($DA_{\mathbf{X2:X5}}$ = -40.0 °C, Table 3).

Duplexes with interstrand zippers of monomers **Y** or **Z**, which feature longer linkers between the pyrene and sugar moieties, are progressively less activated than the **X**-series (i.e., *DA* values less negative, Table 3). This likely reflects less efficient intercalation of the pyrenes. Nonetheless, duplexes with +1 zippers are still strongly activated for dsDNA recognition.

Duplexes with interstrand arrangements of two 2'-*N*-methyl-2'-*N*-(pyren-1-yl)methyl-2'-aminodeoxyuridine **Q** or 2'-*O*-(pyren-1-yl)methyluridine **P** monomers display similar characteristics as the **W**-series (Table 3), including similar *DA* values for +1 zipper duplexes **Q2:Q5** and **P2:P5** as for **W2:W5**, which supports our hypothesis that **Q** and **P** are functional mimics of the original Invader LNA monomer.

Duplexes with interstrand zippers of N2'-acylated 2'-*N*-methyl-2'-aminodeoxyuridine monomers **S** or **V** generally display low thermostability and are moderately activated regardless of the interstrand monomer arrangement (*DA* < 0 °C, Table 3). **S2:S5** and **V2:V5** are the least activated examples of double-stranded probes with +1 zippers of pyrene-functionalized monomers studied herein.

To sum up the thermal denaturation characteristics of DNA duplexes with different interstrand zipper arrangements of pyrene-functionalized monomers, +1 interstrand zippers consistently result in the most pronounced thermal activation of double-stranded probes (i.e., compare *DA* values of **B2:B5** vs other monomer arrangements, Table 3). The level of activation is monomer dependent and decreases in the following order: **X** > **Y** ≥ **Q** ≥ **W** ≥ **P** > **Z** ≥ **S** > **V** (*DA* values for **B2:B5**, Table 3).

Similar trends are observed for duplexes with interstrand zipper arrangements of pyrene-functionalized adenine monomers **K/L/M/R** (Table 4). Thus, duplexes with +1 interstrand zippers display low thermostability and strongly negative *DA* values (see data for **B6:B8** and **B7:B9**, Table 4), while duplexes with +3 or -1 zippers generally are highly thermostable due to additive contributions from both monomers. Moreover, the relationships between *DA* values and linker chemistry/length resemble those observed for the corresponding thymine analogues (trend in *DA* values for +1 zippers: **L** > **M** ≥ **K** vs **X** > **Y** ≥ **W**, Tables 3 and 4). Furthermore, duplexes with +1 zippers of **R** monomers display similar *DA* values as the corresponding duplexes composed of the synthetically more elaborate **K** monomers.

Importantly, the results demonstrate that Invaders can be constructed using pyrimidine, as well as, purine building blocks, which is necessary if sequence-unrestricted recognition of dsDNA is to be realized.

The thermostability of duplexes with 'mixed' interstrand arrangements of N2'-pyrene-functionalized 2'-amino-α-L-LNA adenine monomers **K** and **L** was also evaluated (i.e., one strand modified with monomer **K**, the other strand modified with monomer **L**, Table S2). Briefly described, the observed *DA* values are intermediary of those observed for the corresponding duplexes with zippers composed of only one monomer. For example, duplexes with 'mixed' +1 zippers display *DA* values between -19.5 °C and -23.0 °C. Thus, Invaders can be designed with +1 zippers that are comprised of different monomers, although there is no clear advantage to this approach.

The thermostability of duplexes, in which one strand is modified with a N2'-pyrene-functionalized 2'-amino-α-L-LNA thymine monomer (**W** or **X**) and the other strand is modified with a corresponding adenine monomer (**K** or **L**) was also evaluated (Tables S3-S6). Briefly described: i) duplexes with -2 interstrand zippers are highly thermostable due to additive contributions from both monomers (i.e., ΔT_m's $\gg$ 0 °C and *DA* ~ 0 °C); ii) duplexes with +2 zippers are thermally activated but rather thermostable ($\Delta T_m \gg$ 0 °C; *DA* between -19.0 °C to -10.5 °C); and iii) duplexes with 0-zippers are generally more strongly activated than duplexes with +2 zippers (*DA* between -22.0 °C to -10.0 °C) and vary between being weakly-to-highly thermostable (ΔT_m between -4.5 °C and +12.5 °C). Very similar trends were observed for duplexes in which one strand is modified with a 2'-*O*-

(pyren-1-yl)methyluridine monomer **P** and the other strand is modified with a corresponding adenine monomer **R** (Table S7).

To sum up, duplexes with +1 zippers of pyrene-functionalized monomers are the most strongly activated constructs for dsDNA-recognition via the Invader approach (i.e., lowest *DA* values). While Invaders based on 2'-*N*-(pyren-1-yl)carbonyl-2'-amino-α-L-LNA monomers are most strongly activated, Invaders modified with the synthetically simpler 2'-*N*-methyl-2'-*N*-(pyren-1-yl)methyl-2'-amino-DNA and 2'-*O*-(pyren-1-yl)methyl-RNA monomers also have prominent dsDNA-recognition potential.

Steady-state fluorescence emission spectra of duplexes with interstrand arrangements of pyrene-functionalized monomers

As a first step toward rationalizing the observed thermostability trends, steady-state fluorescence emission spectra of duplexes with different interstrand arrangements of pyrene-functionalized monomers were recorded at 5 °C using an excitation wavelength of λ_{ex} = 350 nm (Fig. 3). Interestingly, duplexes with +1 interstrand monomer arrangements have distinctly different emission profiles than duplexes with other zippers. For example, **W2:W5** and **Y2:Y5** display structured pyrene monomer peaks at λ_{em} ~380 nm and ~400 nm along with a dominant excimer emission at λ_{em} ~ 490 nm, which implies a coplanar arrangement of pyrene moieties with an interplanar separation of ~3.4 Å.[40] Duplexes with +1 zippers of monomers **Q, V, P, M** or **R** display weak pyrene-pyrene excimer emission, in addition to monomer emission (Fig. 3). With the exception of **P1:P4**, duplexes with other interstrand arrangements of pyrene-functionalized monomers display no or minimal excimer emission, indicating that interactions between pyrene moieties are negligible. We speculate that the intense excimer emission of +2 zipper duplex **P1:P4** is a result of pyrene-pyrene stacking interactions in the grooves, in a similar manner as observed for DNA duplexes with +2 zipper arrangements of pyrene-functionalized *ara*-uridine monomers.[41-43] Interestingly, +1 zipper duplexes **X2:X5** and **S2:S5**, which are comprised of (pyren-1-yl)carbonyl-functionalized monomers, do not display excimer emission, but instead feature monomer emission that is considerably more intense than in duplexes with other interstrand arrangements.

There are many reports of duplexes with interstrand zipper arrangements of pyrene-functionalized monomers in which excimer-emitting pyrene dimers are formed in the grooves[41-50] or duplex core.[26,29,31,52-54] Considering that intercalation of the pyrene moieties is expected to be the primary binding mode for the monomers reported herein,[32,34,36,39] stacking of the pyrenes inside the duplex core appears to be the most plausible binding mode for double-stranded probes with +1 interstrand monomer arrangements.

Molecular modeling studies of W2:W5

To gain additional insight into the structural factors that govern the thermal activation of duplexes with +1 interstrand zippers of pyrene-functionalized nucleotides, we performed a molecular modeling study on **W2:W5**. Briefly described, the duplex was initially built with a standard *B*-type helix geometry and subjected to a Monte Carlo search using the AMBER94 force field[55] with the improved parambsc0 parameter set[56] and the GB/SA solvation model[57] as implemented in MacroModel v9.8.[58] Representative examples of the resulting structures were subsequently used as seed structures for stochastic dynamics simulations (5 ns; 300 K) during which structures were collected at regular intervals and energy-minimized. The lowest energy structure obtained via this protocol displays intercalation of one pyrene moiety, while the other is projected into the major groove (Fig. S1). Given that this structure does not account for the observed excimer emission of

W2:W5, we examined structures of higher energy. In one ensemble of structures, the pyrene moieties of both **W** monomers intercalate into the duplex core and engage in mutual stacking interactions (Fig. 4). Specific 3'-directed intercalation of the pyrene moieties results in molecular crowding, duplex extension (*rise* = 10.6 Å), and unwinding (*twist* = 23°, 20° and 24° for A_4T_{15}–$\mathbf{W}_5A_{14}$, $\mathbf{W}_5A_{14}$–$A_6\mathbf{W}_{13}$, and $A_6\mathbf{W}_{13}$–T_7A_{12}; numbering: 5'-$G_1T_2G_3A_4\mathbf{W}_5A_6T_7G_8C_9$ and 3'-$C_{18}A_{17}C_{16}T_{15}A_{14}\mathbf{W}_{13}A_{12}C_{11}G_{10}$) relative to the corresponding unmodified DNA duplex (*rise* = 3.3 Å; *twist* = 31°, 30° and 31°; results not shown). Moreover, the pyrene-pyrene interaction perturbs the stacking interaction between the pyrene and thymine moieties of a **W** monomer (Fig. 4 – upper right). We have previously observed these interactions in modeling structures of singly modified DNA duplexes and proposed them as key factors for the affinity-enhancing properties of **W** monomers.[32] Moreover, the pyrene moieties of **W2:W5** engage in stacking interactions with the 3'-flanking nucleobase on 'their own' strand but interact very little with the thymine of the **W** monomer in the +1 position on the opposite strand. As a result, the flanking base pairs are strongly bent (*buckle* = 20° and -35° for $\mathbf{W}_5A_{14}$ and $A_6\mathbf{W}_{13}$, respectively), relative to the corresponding unmodified DNA duplex (*buckle* = 6° and -4° for T_5A_{14} and A_6T_{13}, respectively).

The structural model of **W2:W5** shown in Figure 4 accounts for the observed excimer emission and thermal activation. The duplex perturbation in the vicinity of the +1 zipper arrangement of the **W** monomers, likely reflects a violation of the 'nearest neighbor exclusion principle', which states that free intercalators - at most - bind to every second base pair of a DNA duplex, due to limits in the local expandability of duplexes.[59] A +1 interstrand arrangement of **W** monomers, results in a localized region with one intercalator per base pair (Fig. 4). Similar structural consequences have been observed in NMR structures of DNA duplexes with adjacent incorporations of pyrene-modified non-nucleotide monomers.[33]

Given the similarities in hybridization and fluorescence emission characteristics, we speculate that duplexes with +1 zipper arrangements of the other pyrene-functionalized monomers studied herein, adopt similar duplex structures.

NMR studies on a DNA duplex with a +1 interstrand zipper of W monomers

Next, we performed NMR studies on a 13-mer DNA duplex with a single +1 interstrand arrangement of **W** monomers to substantiate the structural hypothesis established from molecular modeling (**W13a:W13b**; T_m = 41.0 °C; ΔT_m = +3.5 °C; DA = -17.5 °C, Fig. 5).[31] The 800 MHz ^{1}H NMR spectrum of **W13a:W13b** in 95% H_2O (T = 25 °C) exhibits several imino resonances between δ 12.7 and 13.5 ppm (Fig. 5 – upper panel), which implies formation of Watson-Crick base pairs. However, the low number of observable signals does not fully satisfy the suggested base pairing pattern of **W13a:W13b**. The 2D NOESY spectrum of **W13a:W13b** confirms that complementary duplexes are formed in solution (Fig. S2). However, NMR resonances assigned to nucleotides near monomer **W** get progressively broader, and signals of protons that are spatially close to the pyrene moieties are not observed at all (Fig. 5 – lower panel). Thus, no aromatic or sugar resonances could be observed for residues W5-T7 and W8-T10 in the **W13a** and **W13b** strands, respectively; also, the T3 and T9 imino resonances of the **W13a** strand and T6 imino resonance of the **W13b** strand exhibit considerable broadening (Fig. 5 – upper panel inset). Several magnetic fields, fast and slow annealing procedures, and temperatures ranging from 0 to 35 °C were explored in unsuccessful attempts to observe the missing resonances. Temperature variation only resulted in minor changes in ^{1}H chemical shifts and peak intensities.

Hence, the results substantiate that +1 interstrand zippers of **W** monomers induce significant local perturbation of probe duplexes, which explains their relatively low thermostability.

Invader-mediated recognition of DNA hairpins

Next, we examined dsDNA-targeting characteristics of double-stranded probes with interstrand arrangements of pyrene-functionalized monomers. Assuming that efficient recognition of dsDNA targets requires probes that are thermally activated and display low thermostability (i.e., $DA \ll 0$ °C and $\Delta T_m \leq 0$ °C), we decided to focus our efforts on probes with +1 interstrand monomer arrangements.

In our original studies, we demonstrated - using fluorescence-based assays - that **W**-modified Invaders efficiently recognize 9- and 13-mer dsDNA targets at conditions designed to minimize strand exchange between probes and targets ($[Na^+]$ = 110-710 mM; $T_{experimental} < T_m$).[29,31] To evaluate Invaders in a more challenging assay, we recently introduced an electrophoretic mobility shift based assay,[37] a version of which is used herein. Thus, a digoxigenin (DIG) labeled DNA hairpin (DH) - comprised of a 9-mer double-stranded stem, linked together via a T_{10} loop - serves as the model dsDNA target (Figs. 6a and 6b). The unimolecular nature of the DNA hairpin, confers significant stability to the stem region [T_m (**DH1**) = 56.0 °C vs T_m (**D1:D2**) = 29.5 °C]. Invader-mediated binding to the DNA hairpin is expected to form recognition complexes with lower electrophoretic mobility on non-denaturing PAGE gels than unreacted DNA hairpins (Fig. 6a).

Indeed, incubation of Invader LNA **W2:W5** with DNA hairpin **DH1** (~3h, rt) results in dose-dependent formation of slower moving recognition complexes (Fig. 6c). While only trace amounts of complex are observed when a 5-fold molar excess of **W2:W5** is used, ~50% mixed-sequence recognition is realized with 100-fold excess (Fig. 6c; Table 5; Fig. S3). Interestingly, moderately activated Invaders display poor recognition efficiency (i.e., **S2:S5, V2:V5, K6:K8** and **M6:M8**; $DA \geq -21$ °C; < 20% recognition at 100-fold excess, Table 5), whereas strongly activated Invaders recognize DNA hairpins with high and remarkably similar efficiency (i.e., $DA < -21$ °C; 40-50% recognition at 100-fold excess; Figs. 6c and 6d; Table 5; Figs. S3 and S4). The latter group includes Invaders modified with N2'-pyrene-functionalized 2'-amino-α-L-LNA **X** or **Y** monomers, synthetically less elaborate **P** or **Q** monomers, and adenine monomer **R**. Importantly, none of the following control experiments produced appreciable amounts of recognition complexes:[60] a) incubation of up to 500-fold excess of unmodified DNA duplex **D1:D2** with DNA hairpin **DH1** (Fig. 6e); b) incubation of 100-fold excess of single-stranded **W2/W5/Q2/Q5/P2/P5/R6/R8** with DNA hairpin **DH1** (Fig. 6f and Fig. S5); and c) incubation of 100-fold excess of selected Invaders **W2:W5, Q2:Q5, X2:X5, Y2:Y5** or **K6:K8** with DNA hairpins **DH2** or **DH3** featuring fully base-paired but non-isosequential stem regions [one or two base pair deviations relative to Invaders; T_m (**DH2**) = 57.0 °C; T_m (**DH3**) = 64.5 °C] (Fig. 6g-h and Fig. S6).

Thus, the results demonstrate that Invaders - composed of a variety of pyrene-functionalized nucleotides - can recognize the double-stranded stems of DNA hairpins. The control experiments show that i) the energetic hotspots play a critical role in activating Invaders for mixed-sequence dsDNA-recognition, ii) both strands of an Invader probe are required for the recognition to take place, and iii) Invader-mediated dsDNA-recognition proceeds with excellent binding specificity. Given the important roles that DNA hairpins play in the regulation of gene expression,[61,62] hairpin-targeting Invaders can be envisioned as molecular tools for the study of these processes. While the DNA hairpins studied here represent a lower level of complexity than long DNA duplexes and dsDNA in tightly packaged chromatin, we are very encouraged to note that second-generation Invaders

already have been shown to recognize mixed-sequence chromosomal DNA regions in the context of non-denaturing FISH experiments.[37]

Conclusion

In the present study we demonstrate that incorporation of +1 interstrand zippers of intercalator-functionalized nucleotides is a general strategy to activate double-stranded probes for mixed-sequence dsDNA-recognition via a dual duplex invasion mechanism, which relies on differences in thermostability between probes and probe-target duplexes. Our structural studies strongly suggest that Invaders are destabilized by the duplex distortion that ensues when two intercalating pyrene moieties, positioned in a +1 zipper, are competing for the same region in the duplex core. Importantly, we demonstrate that the key features of these 'energetic hotspots' can be emulated using 2'-*O*-(pyren-1-yl)methyl-RNA or 2'-*N*-methyl-2'-*N*-(pyren-1-yl)methyl-2'-amino-DNA monomers. Thus, Invaders modified with these building blocks recognize DNA hairpins with similar efficiency as Invaders based on the original 2'-*N*-(pyren-1-yl)methyl-2'-amino-α-L-LNA monomers. Identification of synthetically simple - yet efficient - monomers represents an important practical advance, which will facilitate systematic structure-property studies and accelerate the use of Invaders for applications in molecular biology and nucleic acid diagnostics. In fact, second-generation Invaders have already been demonstrated to recognize mixed-sequence chromosomal DNA regions in the context of non-denaturing FISH experiments.[37] Studies aiming at further refining the Invader approach into a general strategy for mixed-sequence recognition of dsDNA are ongoing and will be reported shortly.

Experimental section

Synthesis of functionalized oliogonucleotides

The vast majority of the ONs used in the present study, have been prepared and characterized with respect to identity (MALDI-MS) and purity (>80%, ion-pair reverse-phase HPLC) in conjunction with previous studies.[32,34,38,39] **P3** was synthesized in a similar fashion as other **P**-modified ONs.[34] Novel ONs **R6**-**R9**, which are modified with the 2'-*O*-(pyren-1-yl)methyladenosine monomer **R**,[63] were synthesized via machine-assisted solid-phase DNA synthesis (0.2 μmol scale; 500 Å succinyl linked LCAA-CPG support) using extended coupling times (4,5-dicyanoimidazole as activator, 15 min, ~98% coupling yield) during incorporation of the corresponding A^{Bz}-protected phosphoramidite of monomer **R**. The ONs were worked up, purified by RP-HPLC, and characterized with respect to identity (MALDI-MS) and purity (>80%, ion-pair reverse-phase HPLC) following our standard protocols.[34]

Thermal denaturation studies

The concentrations of all ONs were estimated using the following extinction coefficients ($L \times mmol^{-1} \times cm^{-1}$) at 260 nm: dA (15.20), dC (7.05), dG (12.01), T (8.40); pyrene (22.40). ONs (1.0 μM each strand) were thoroughly mixed in T_m-buffer (see below), denatured by heating and subsequently cooled to the starting temperature of the experiment. Thermal denaturation curves (A_{260} vs T) were recorded using a UV/VIS spectrometer equipped with a Peltier temperature programmer. The temperature was varied from at least 15 °C below to 15 °C above the thermal denaturation temperature using a ramp of 0.5 °C min^{-1}. Quartz optical cells with a path-length of 10 mm were used. A medium salt T_m-buffer was used (100 mM NaCl, 0.1 mM EDTA, pH 7.0 adjusted with 10 mM NaH_2PO_4 and 5 mM Na_2HPO_4). Thermal denaturation temperatures were determined from the first derivative of thermal denaturation curves using the software provided with the UV/VIS spectrometer.

Reported thermal denaturation temperatures were determined as an average from two separate experiments within ±1.0 °C.

Molecular modeling protocol

An unmodified DNA duplex was built in a standard *B*-type geometry and subsequently modified within MacroModel v9.8[58] to provide a starting structure of **W2:W5**. The charge of the phosphodiester backbone was neutralized with sodium ions, which were placed 3.0 Å from the two non-bridging oxygen atoms. The starting structure was then subjected to a Monte Carlo conformational search. The conformational space was sampled by varying the N2'-CH_2 and CH_2-$C1_{Py}$ torsion angles of monomers **W**; 55998 structures were generated and minimized using the AMBER94 force field[55] with the improved parambsc0 parameter set[56] and the GB/SA solvation model[57] and Polak-Ribiere conjugate gradient method (convergence criteria 0.1 kJ/mol×Å) as implemented in MacroModel V9.8.[58] The original AMBER94 parameters were used for monomer **W** and the 3'-neighboring nucleotide. Non-bonded interactions were treated with extended cut-offs (van der Waals 8.0 Å and electrostatics 20.0 Å). All atoms were allowed to move freely during minimization, except for the following distance restraints: a) sodium ions were restrained to 3.0 Å from the two non-bridging oxygen atoms of the corresponding phosphodiester groups by a force constant of 100 kJ/mol×$Å^2$, and b) hydrogen bonding distances between the thymine moiety of monomer **W** and its Watson-Crick partner [(T)N3-H···N1(A), distance 1.85 Å and (T)4-O···HN-6(A), distance 1.81 Å], as well as of the outermost base pairs [(C)2-O···HN-2(G), distance 1.98 Å, (C)N3···H-N1(G), distance 1.94 Å and (C)4-NH···O-6(G), distance 1.89 Å] were restrained by a force constant of 100 kJ/mol×$Å^2$. Twelve representative low-energy structures were subsequently submitted to 5 ns of stochastic dynamics (simulation temperature 300 K; time step 2.2 fs; SHAKE all bonds to hydrogen; same distance restraints as during Monte Carlo search) during which 500 structures were sampled at regular time intervals to allow conformational analysis and energy minimization (convergence criteria 0.05 kJ/mol·Å).

NMR spectroscopy

Equimolar amounts of **W13a** and **W13b** were dissolved in 95% H_2O, 5% ^2H_2O with the addition of NaCl (50 mM) and Na-phosphate buffer (pH 6.7). All NMR spectra were acquired on 800 or 600 MHz NMR spectrometers equipped with cold or room temperature triple probes, respectively. 2D NOESY spectra were used for the sequential assignment and were acquired with τ_m values of 80, 150 and 250 ms. 2D TOCSY spectra were used for the identification of pyridine H5 resonances and were acquired with 80 ms τ_m (data not shown). All experiments were performed on a natural abundance sample at temperatures ranging from 0 to 35 °C. NMR spectra were processed and analyzed using VNMRJ (Varian Inc.) and Sparky software (UCSF).

Invader-mediated recognition of DNA hairpins - electrophoretic mobility shift assays

This assay, which was conducted *in lieu* of footprinting experiments to avoid the use of ^{32}P-labeled targets, was performed in a similar manner as previously described.[37] Thus, ~100 pmols of unmodified **DH1-DH3** were 3'-DIG-labeled using the 2nd generation DIG Gel Shift Kit (Roche Applied Bioscience) as recommended. Equal volumes of 100 nM solution of DIG-labeled dsDNA targets and probe solution (concentrations: 0.5 μM, 1 μM, 5 μM, 10 μM, 50 μM) in 1X HEPES buffer (50 mM HEPES, 100 mM NaCl, 5 mM $MgCl_2$, pH 7.2, 10 % sucrose, 1 mg/mL spermine tetrahydrochloride) were mixed and incubated for 3h at room temperature, before being loaded on a 15% non-denaturing polyacrylamide gel. After 2-3 h of electrophoresis at 100V in a cold room (~4 °C), the nucleic acid complexes were transferred to a positively charged nylon membrane by electroblotting, and processed as

recommend by the manufacturer of the DIG Gel Shift Kit. The chemiluminescence was captured on an X-ray film and the bands were quantified using Quantity One software.

Supplementary Material

Refer to Web version on PubMed Central for supplementary material.

Acknowledgments

This study was supported by Award Number R01 GM088697 from the National Institute Of General Medical Sciences, National Institutes of Health; Award Number IF13-001 from the Higher Education Research Council, Idaho State Board of Education; Idaho NSF EPSCoR; the BANTech Center at Univ. Idaho; the Slovenian Research Agency (ARRS, P1-0242 and J1-4020); the Danish National Research Foundation; and the Danish Agency for Science Technology and Innovation.

References and notes

1. Rogers FA, Lloyd JA, Glazer PM. Curr Med Chem : Anti-Cancer Agents. 2005; 5:319–326.
2. Ghosh I, Stains CI, Ooi AT, Segal DJ. Mol BioSyst. 2006; 2:551–560. [PubMed: 17216036]
3. Nielsen PE. ChemBioChem. 2010; 11:2073–2076. [PubMed: 20872391]
4. Mukherjee A, Vasquez KM. Biochimie. 2011; 93:1197–1208. [PubMed: 21501652]
5. Aiba Y, Sumaoka J, Komiyama M. Chem Soc Rev. 2011; 40:5657–5668. [PubMed: 21566825]
6. Vaijayanthi T, Bando T, Pandian GN, Sugiyama H. ChemBioChem. 2012; 13:2170–2185. [PubMed: 23023993]
7. Simon P, Cannata F, Concordet J-P, Giovannangeli C. Biochimie. 2008; 90:1109–1116. [PubMed: 18460344]
8. Duca M, Vekhoff P, Oussedik K, Halby L, Arimondo PB. Nucleic Acids Res. 2008; 36:5123–5138. [PubMed: 18676453]
9. Kaihatsu K, Janowski BA, Corey DR. Chem Biol. 2004; 11:749–758. [PubMed: 15217608]
10. Nielsen PE. Chem Biodiversity. 2010; 7:786–804.
11. Dervan PB, Edelson BS. Curr Opin Struct Biol. 2003; 13:284–299. [PubMed: 12831879]
12. Kutyavin IV, Rhinehart RL, Lukhtanov EA, Gorn VV, Meyer RB Jr, Gamper HB Jr. Biochemistry. 1996; 35:11170–11176. [PubMed: 8780521]
13. Lohse J, Dahl O, Nielsen PE. Proc Natl Acad Sci. 1999; 96:11804–11808. [PubMed: 10518531]
14. Ishizuka T, Yoshida J, Yamamoto Y, Sumaoka J, Tedeschi T, Corradini R, Sforza S, Komiyama M. Nucleic Acids Res. 2008; 36:1464–1471. [PubMed: 18203747]
15. Janowski BA, Kaihatsu K, Huffman KE, Schwartz JC, Ram R, Hardy D, Mendelson CR, Corey DR. Nat Chem Biol. 2005; 1:210–215. [PubMed: 16408037]
16. Beane R, Gabillet S, Montaillier C, Arar K, Corey DR. Biochemistry. 2008; 47:13147–13149. [PubMed: 19053275]
17. Rapireddy S, Bahal R, Ly DH. Biochemistry. 2011; 50:3913–3918. [PubMed: 21476606]
18. Bahal R, Sahu B, Rapireddy S, Lee C-M, Ly DH. ChemBioChem. 2012; 13:56–60. [PubMed: 22135012]
19. Rusling DA, Powers VEC, Ranasinghe RT, Wang Y, Osborne SD, Brown T, Fox K. Nucleic Acids Res. 2005; 33:3025–3032. [PubMed: 15911633]
20. Hari Y, Obika S, Imanishi T. Eur J Org Chem. 2012:2875–2887.
21. Bogdanove AJ, Voytas DF. Science. 2011; 333:1843–1846. [PubMed: 21960622]
22. Gaj T, Gersbach CA, Barbas CF III. Trends Biotechnol. 2013; 31:397–405. [PubMed: 23664777]
23. Tse WC, Boger DL. Chem Biol. 2004; 11:1607–1617. [PubMed: 15610844]
24. Hamilton PL, Arya DP. Nat Prod Rep. 2012; 29:134–143. [PubMed: 22183179]
25. Bryld T, Højland TR, Wengel J. Chem Commun. 2004:1064–1065.
26. Filichev VV, Vester B, Hansen LH, Pedersen EB. Nucleic Acids Res. 2005; 33:7129–7137. [PubMed: 16377781]

27. Ge R, Heinonen JE, Svahn MG, Mohamed AJ, Lundin KE, Smith CIE. FASEB J. 2007; 21:1902–1914. [PubMed: 17314142]
28. Moreno PMD, Geny S, Pabon YV, Bergquist H, Zaghloul EM, Rocha CSJ, Oprea II, Bestas B, Andaloussi SEL, Jørgensen PT, Pedersen EB, Lundin KE, Zain R, Wengel J, Smith CIE. Nucleic Acids Res. 2013; 41:3257–3273. [PubMed: 23345620]
29. Hrdlicka PJ, Kumar TS, Wengel J. Chem Commun. 2005:4279–4281.
30. The following nomenclature describes the relative arrangement between two monomers positioned on opposing strands in a duplex. The number *n* describes the distance measured in number of base pairs and has a positive value if a monomer is shifted toward the 5'-side of its own strand relative to a second reference monomer on the other strand, or a negative value if a monomer is shifted toward the 3'-side of its own strand relative to a second reference monomer on the other strand.
31. Sau SP, Kumar TS, Hrdlicka PJ. Org Biomol Chem. 2010; 8:2028–2036. [PubMed: 20401378]
32. Kumar TS, Madsen AS, Østergaard ME, Sau SP, Wengel J, Hrdlicka P. J Org Chem. 2009; 74:1070–1081. [PubMed: 19108636]
33. Nielsen CB, Petersen M, Pedersen EB, Hansen PE, Christensen UB. Bioconjugate Chem. 2004; 15:260–269.
34. Karmakar S, Anderson BA, Rathje RL, Andersen S, Jensen T, Nielsen P, Hrdlicka PJ. J Org Chem. 2011; 76:7119–7131. [PubMed: 21827174]
35. Kalra N, Babu BR, Parmar VS, Wengel J. Org Biomol Chem. 2004; 2:2885–2887. [PubMed: 15480448]
36. Nakamura M, Fukunaga Y, Sasa K, Ohtoshi Y, Kanaori K, Hayashi H, Nakano H, Yamana K. Nucleic Acids Res. 2005; 33:5887–5895. [PubMed: 16237124]
37. Didion BA, Karmakar S, Guenther DC, Sau SP, Verstegen JP, Hrdlicka PJ. ChemBioChem. 2013; 4:3447–3454.
38. Kumar TS, Madsen AS, Wengel J, Hrdlicka PJ. J Org Chem. 2006; 71:4188–4201. [PubMed: 16709060]
39. Andersen NK, Wengel J, Hrdlicka PJ. Nucleosides Nucleotides Nucleic Acids. 2007; 26:1415–1417. [PubMed: 18066795] . (b) synthesis of monomer **M** will be published elsewhere.
40. Winnik FM. Chem Rev. 1993; 93:587–614.
41. Dioubankova NN, Malakhov AD, Stetsenko DA, Gait MJ, Volynsky PE, Efremov RG, Korshun VA. ChemBioChem. 2003; 4:841–847. [PubMed: 12964158]
42. Astakhova IV, Malakhov AD, Stepanova IA, Ustinov AV, Bondarev SL, Paramonov AS, Korshun VA. Bioconjugate Chem. 2007; 18:1972–1980.
43. Astakhova IV, Ustinov AV, Korshun VA, Wengel J. Bioconjugate Chem. 2011; 22:533–539.
44. Hrdlicka PJ, Babu BR, Sørensen MD, Wengel J. Chem Commun. 2004:1478–1479.
45. Hwang GT, Seo YJ, Kim BH. Tetrahedron Lett. 2005; 46:1475–1477.
46. Grünewald C, Kwon T, Piton N, Förster U, Wachtveitl J, Engels JW. Bioorg Med Chem. 2008; 16:19–26. [PubMed: 17512739]
47. Nakamura M, Murakami Y, Sasa K, Hayashi H, Yamana K. J Am Chem Soc. 2008; 130:6904–6905. [PubMed: 18473465]
48. Astakhova IV, Lindegaard D, Korshun VA, Wengel J. Chem Commun. 2010; 46:8362–8364.
49. Seela F, Ingale SA. J Org Chem. 2010; 75:284–295. [PubMed: 20000692]
50. Ingale SA, Pujari SS, Sirivolu VR, Ding P, Xiong H, Mei H, Seela F. J Org Chem. 2012; 77:188–199. [PubMed: 22129276]
51. Kumar PK, Shaikh KI, Jørgensen AS, Kumar S, Nielsen P. J Org Chem. 2012; 77:9562–9573. [PubMed: 23039223]
52. Langenegger SM, Häner R. Chem Commun. 2004:2792–2793.
53. Haner R, Garo F, Wenger D, Malinovskii VL. J Am Chem Soc. 2010; 132:7466–7471. [PubMed: 20459110]
54. Wojciechowski F, Lietard J, Leumann CJ. Org Lett. 2012; 14:5176–5179. [PubMed: 23025305]
55. Cornell WD, Cieplak P, Bayly CI, Gould IR, Merz KM, Ferguson DM, Spellmeyer DC, Fox T, Caldwell JW, Kollman PA. J Am Chem Soc. 1995; 117:5179–5197.

56. Pérez A, Marchán I, Svozil D, Sponer J, Cheatham TE, Laughton CA, Orozco M. Biophys J. 2007; 92:3817–3829. [PubMed: 17351000]
57. Still WC, Tempczyk A, Hawley RC, Hendrickson T. J Am Chem Soc. 1990; 112:6127–6129.
58. MacroModel, version 9.8. Schödinger, LLC; New York, NY: 2010.
59. Chothers DM. Biopolymers. 1968; 6:575–584. [PubMed: 5644787]
60. For additional validation of this assay, please see reference 37.
61. Wadkins RM. Curr Med Chem. 2000; 7:1–15. [PubMed: 10637354]
62. Keene FR, Smith JA, Collins JG. Coord Chem Rev. 2009; 253:2021–2035.
63. Nakamura M, Shimomura Y, Ohtoshi Y, Sasa K, Hayashi H, Nakano H, Yamana K. Org Biomol Chem. 2007; 5:1945–1951. [PubMed: 17551644]

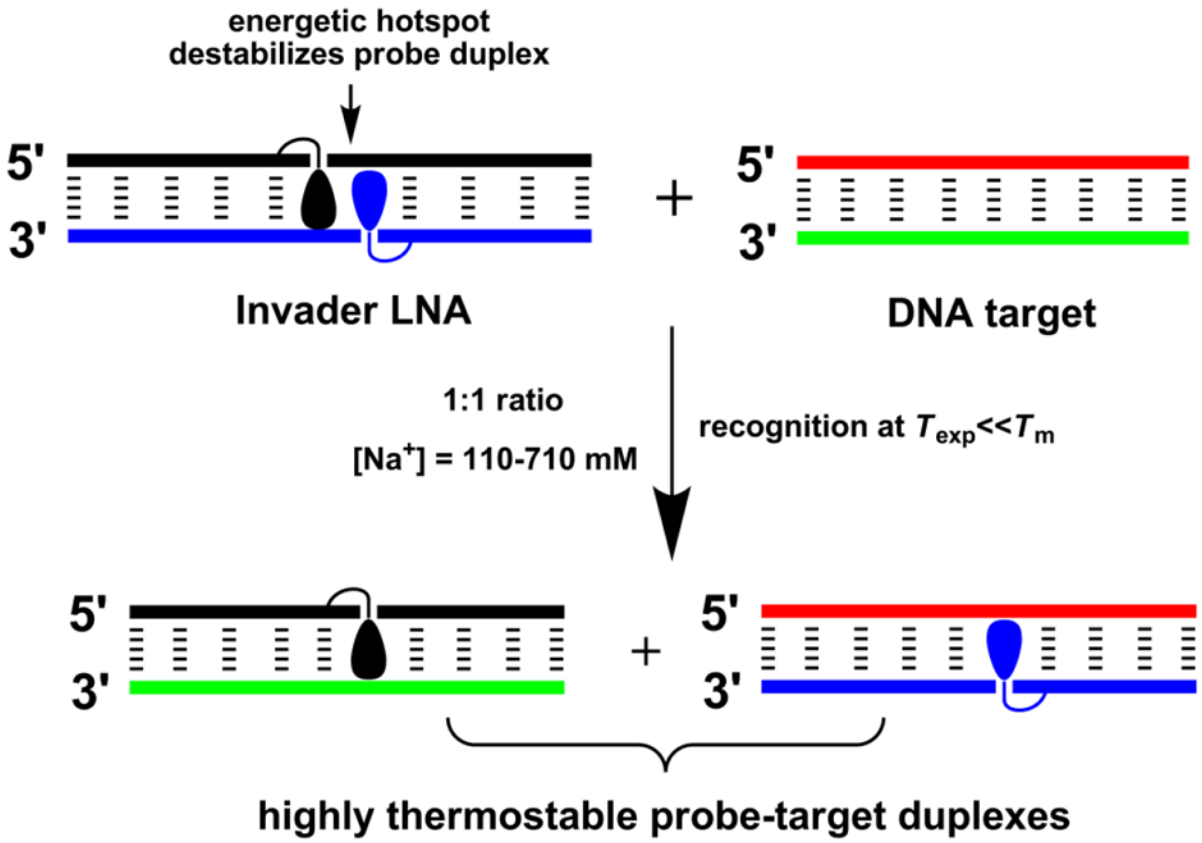

Figure 1.
Illustration of the Invader approach for mixed-sequence recognition of dsDNA. Droplet denotes an intercalating pyrene moiety.

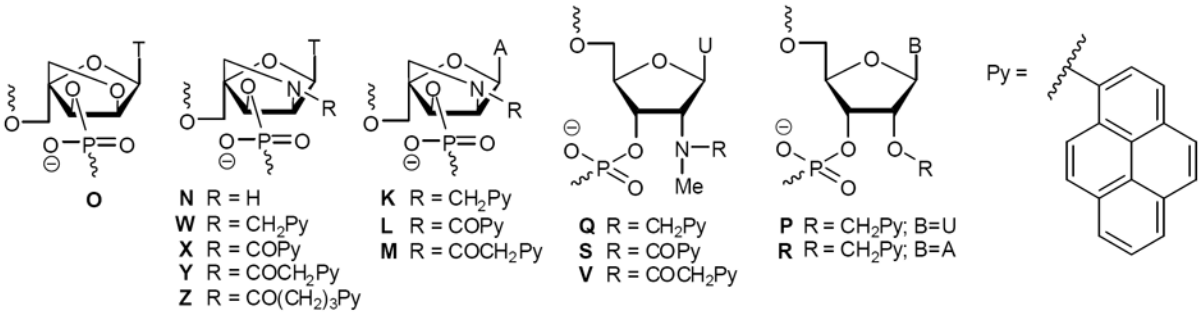

Figure 2.
Structures of monomers studied herein.

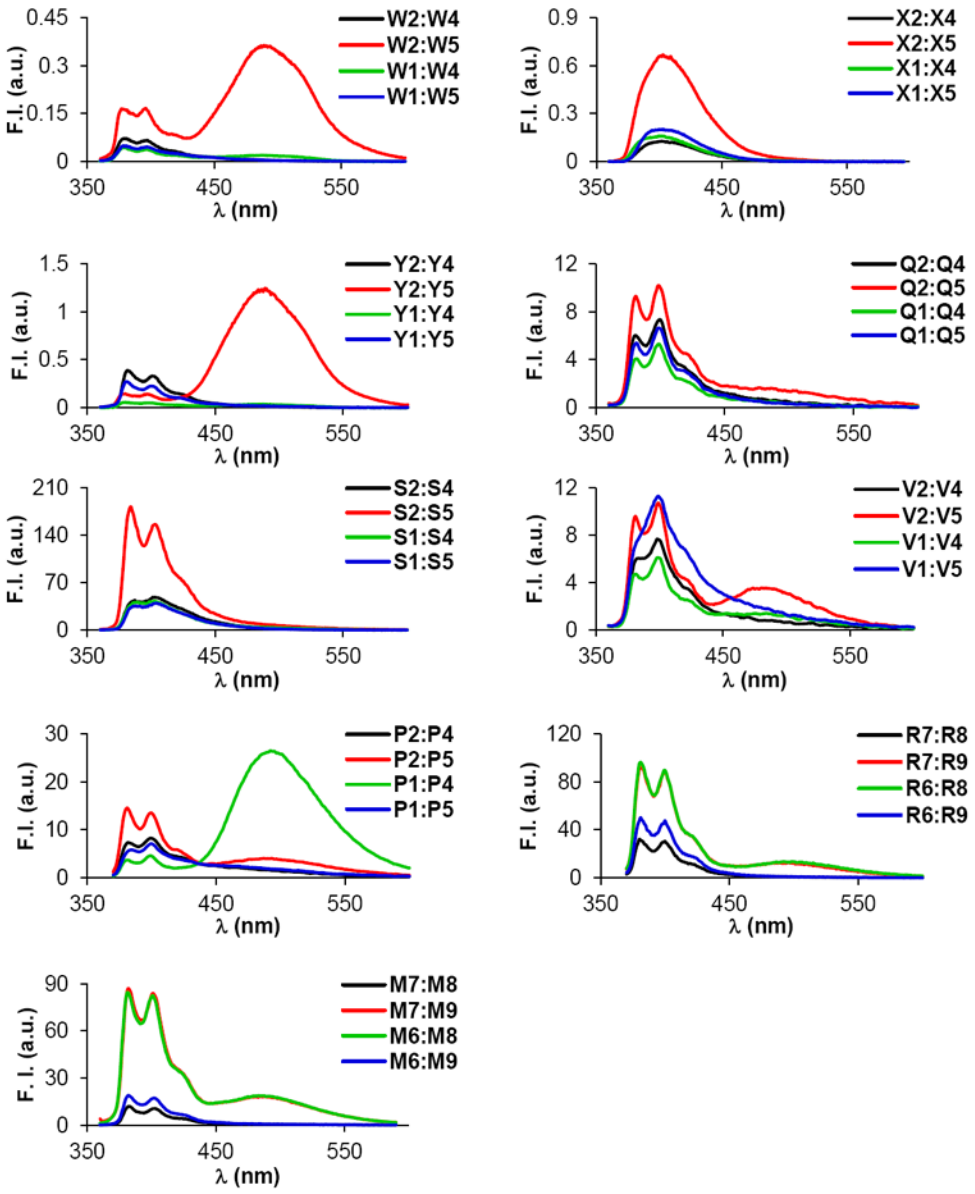

Figure 3.

Steady-state fluorescence emission spectra of duplexes with different interstrand arrangements of selected pyrene-functionalized monomers. Recorded in thermal denaturation buffer at T = 5 °C using 1.0 μM of each strand and λ_{ex} = 350 nm. Please note that different Y-axis scales are used.

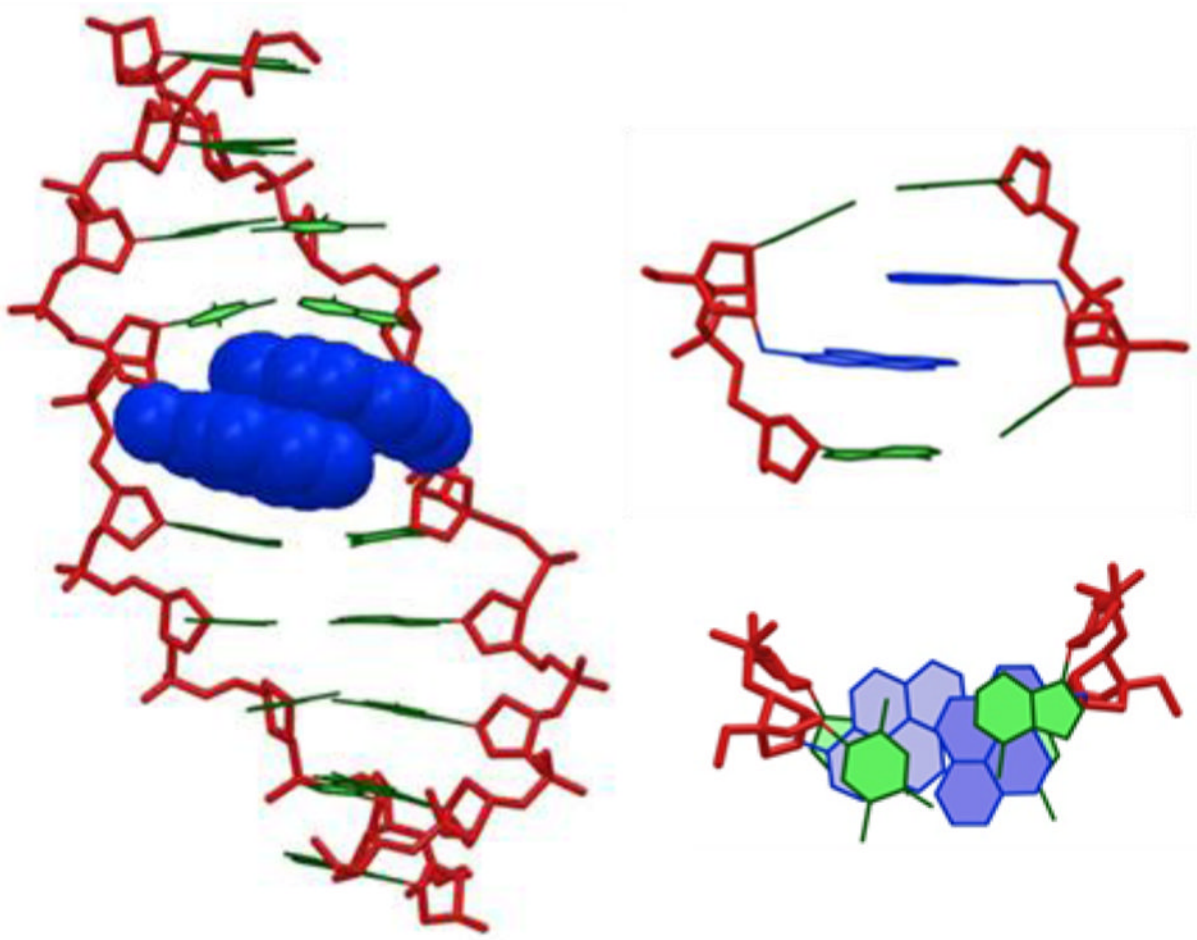

Figure 4.

Energy minimized structure of **W2:W5**. Left: side view of duplex; upper right: alternative representation of the central duplex region; bottom right: top view of the central duplex region. Color code: sugar phosphate backbone (red); pyren-1-ylmethyl moieties of **W** monomers (blue); nucleobases (green). Hydrogen atoms, sodium ions and bond orders are omitted for clarity.

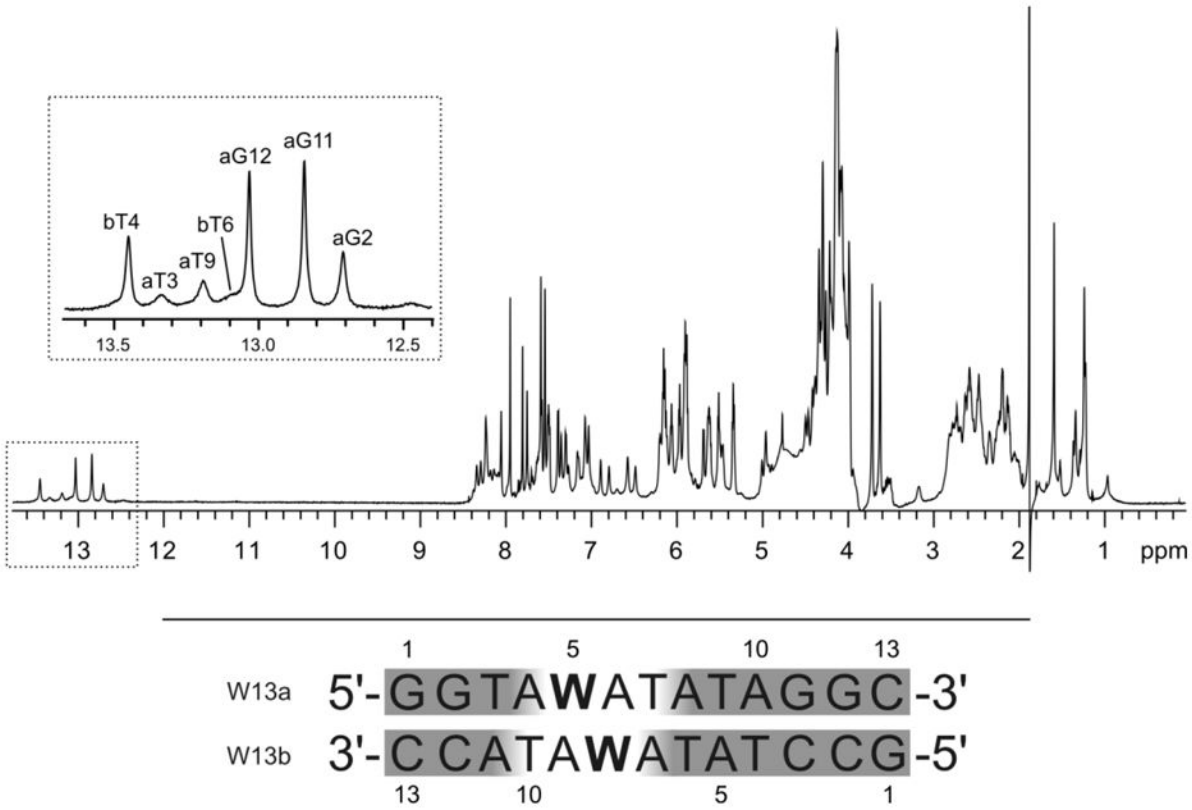

Figure 5.

Upper panel: ^{1}H NMR spectrum of **W13a:W13b** recorded in 95% H_2O at 25 °C. The assignment of imino resonances is shown in the inset with the first letter of assignment indicating either the **a** or **b** strand of the duplex. Lower panel: sequences of **W13a:W13b** and numbering of nucleotides; shaded nucleotides denote regions with observable NMR signals.

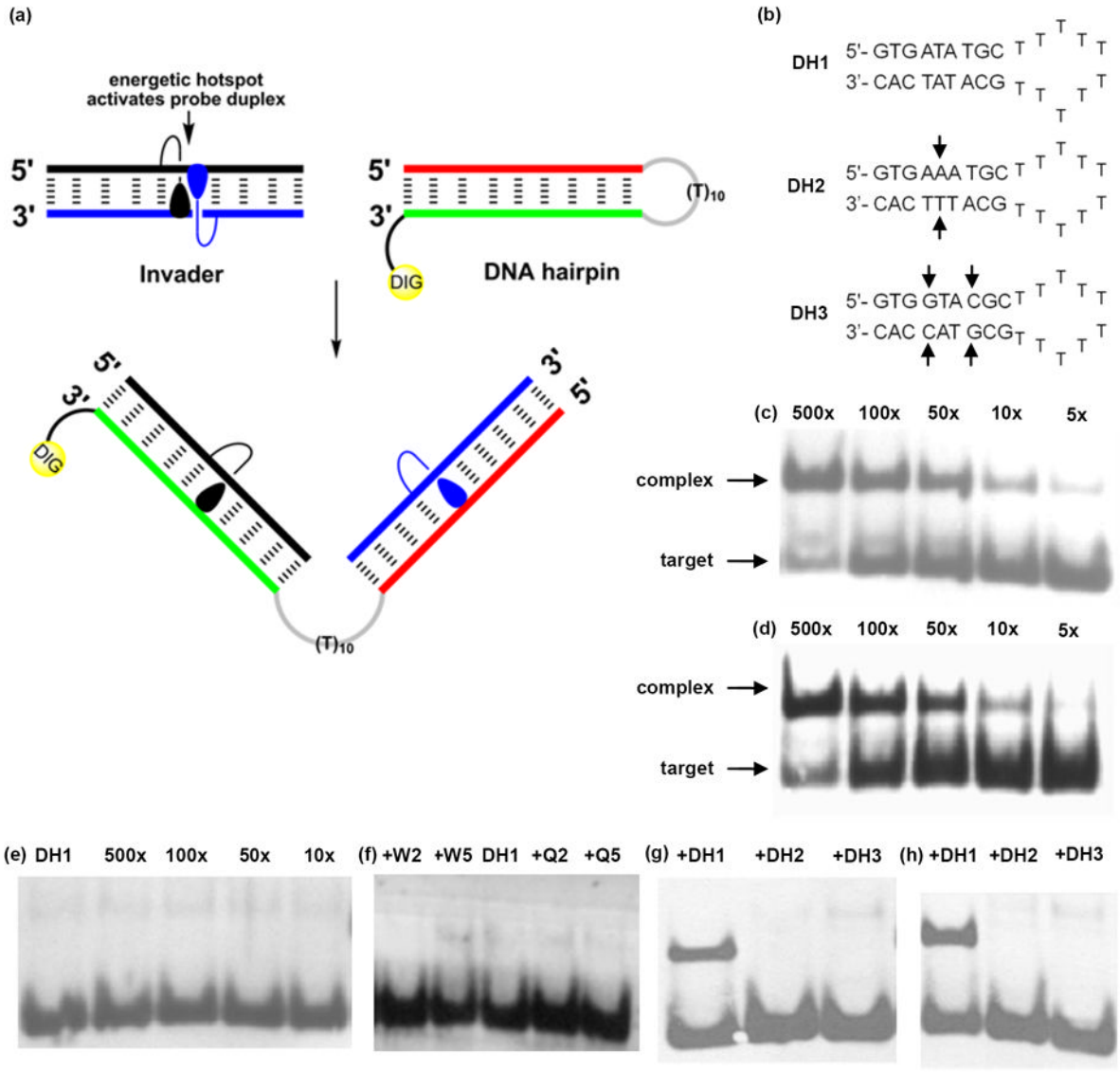

Figure 6.

Recognition of structured dsDNA targets by Invader probes using electrophoretic mobility shift assays. (a) Illustration of recognition process; (b) structures of DNA hairpins with isosequential (**DH1**) or non-isosequential (**DH2** and **DH3**) stem regions (arrows denote points of deviation); (c), (d) and (e): incubation of **DH1** with varying excess of **W2:W5, Q2:Q5** or **D1:D2**, respectively; (f) incubation of **DH1** with 100-fold excess of single-stranded **W2, W5, Q2** or **Q5**; (g) and (h) incubation of **DH1-DH3** with 100-fold excess of **W2:W5** or **Q2:Q5**, respectively. Probe-target incubation: 3h at 20 °C; 15% non-denaturing PAGE; DIG: digoxigenin.

Table 1

ΔT_m values of duplexes between ONs modified with pyrene-functionalized thymine/uracil monomers and complementary DNA, measured relative to unmodified duplexes.[a]

		ΔT_m/°C									
ON	**Duplex**	**B =**	**O**[b]	**N**[b]	**W**[b]	**X**[b]	**Y**[b]	**Z**[b]	**Q**[c]	**S**[c]	**V**[c]	**P**[c]
B1	5′-G**B**G ATA TGC	+2.5	-2.0	+7.0	+10.0	+10.5	+0.5	+5.0	-6.0	-0.5	+5.0
D2	3′-CAC TAT ACG										
B2	5′-GTG A**B**A TGC	+6.0	+0.5	+14.0	+19.0	+15.5	+6.0	+14.0	+3.0	+6.0	+12.5
D2	3′-CAC TAT ACG										
B3	5′-GTG ATA **B**GC	+3.0	-1.0	+10.5	+14.0	+11.5	-	-	-	-	+8.0[d]
D2	3′-CAC TAT ACG										
D1	5′-GTG ATA TGC	+3.5	-0.5	+6.5	+10.5	+10.0	+0.5	+1.5	-6.0	+1.0	+3.5
B4	3′-CAC **B**AT ACG										
D1	5′-GTG ATA TGC	+8.0	+2.5	+15.5	+19.5	+16.5	+6.5	+13.0	+4.0	+6.5	+11.5
B5	3′-CAC TA**B** ACG										

[a] ΔT_m = change in T_m's relative to unmodified reference duplex **D1:D2** ($T_m \equiv 29.5$ °C); T_m's determined as the first derivative maximum of denaturation curves (A_{260} vs T) recorded in medium salt buffer ($[Na^+] = 110$ mM, $[Cl^-] = 100$ mM, pH 7.0 (NaH_2PO_4/Na_2HPO_4)), using 1.0 μM of each strand. T_m values are averages of at least two measurements within 1.0 °C; A = adenin-9-yl-DNA monomer, C = cytosin-1-yl-DNA monomer, G = guanin-9-yl-DNA monomer, T = thymin-1-yl-DNA monomer. See Figure 1 for structures of monomers. "-" = not determined.

[b] Previously reported in reference 32.

[c] Previously reported in reference 34.

[d] Not previously reported.

J Org Chem. Author manuscript; available in PMC 2014 October 04.

Table 2

ΔT_m values of duplexes between ONs modified with pyrene-functionalized adenine monomers and complementary DNA, measured relative to unmodified duplexes.[a]

		ΔT_m /°C				
ON	**Duplex**	**B =**	**K**[b]	**L**[b]	**M**	**R**
B6	5′-GTG **B**TA TGC	+5.0	+11.0	+6.0	+4.5	
D2	3′-CAC TAT ACG					
B7	5′-GTG AT**B** TGC	+7.0	+14.0	+7.5	+8.5	
D2	3′-CAC TAT ACG					
D1	5′-GTG ATA TGC	+6.5	+11.5	+7.5	+8.5	
B8	3′-CAC T**B**T ACG					
D1	5′-GTG ATA TGC	+5.5	+12.0	+6.0	+6.5	
B9	3′-CAC TAT **B**CG					

[a] ΔT_m = change in T_m values relative to unmodified reference duplex **D1:D2** ($T_m \equiv 29.5$ °C); see Table 1 for experimental conditions; see Figure 1 for structures of monomers.

[b] reference 39

Table 3

ΔT_m and *DA* values for DNA duplexes with different interstrand zipper arrangements of thymine/uracil monomers.[a]

			$\Delta T_m[DA]$/°C									
ON	**Zipper**	**Duplex**	**B =**	**O**	**N**	**W**[b]	**X**	**Y**	**Z**	**Q**	**S**	**V**	**P**
B1	+4	5′-G**B**G ATA TGC		+11.0 [+0.5]	+1.0 [+0.5]	+25.0 [+2.5]	+28.5 [-1.0]	+26.0 [-1.0]	+8.5 [+1.5]	+19.5 [+1.5]	-3.5 [-5.5]	+9.0 [+3.0]	+16.5 [0.0]
B5		3′-CAC TA**B** ACG											
B1	+2	5′-G**B**G ATA TGC		+8.0 [+2.0]	-1.5 [+1.0]	0.0 [-13.5]	+6.5 [-14.0]	+12.5 [-8.0]	-1.0 [-2.0]	-1.5 [-8.0]	-17.5 [-5.5]	-2.0 [-2.5]	-6.0 [-14.5]
B4		3′-CAC **B**AT ACG											
B2	+1	5′-GTG A**B**A TGC		+16.0 [+2.0]	-5.5 [-8.5]	+2.5 **[-27.0]**	-1.5 **[-40.0]**	+1.0 **[-31.0]**	-5.5 **[-18.0]**	-2.0 **[-29.0]**	-10.0 **[-17.0]**	+0.5 **[-12.0]**	-2.0 **[-26.0]**
B5		3′-CAC TA**B** ACG											
B2	-1	5′-GTG A**B**A TGC		+7.0 [+2.5]	-5.5 [-5.5]	+15.5 [-5.0]	+26.0 [-3.5]	+26.5 [+1.0]	+9.5 [+3.0]	+13.0 [-2.5]	-8.5 [-5.5]	+5.5 [-2.5]	+10.5 [-5.5]
B4		3′-CAC **B**AT ACG											
B3	-1	5′-GTG ATA **B**GC		+8.5 [-2.5]	-2.5 [-4.0]	+18.0 [-8.0]	+25.0 [-8.5]	+29.5 [+1.5]	-	-	-	-	+14.0 [-5.5]
B5		3′-CAC TA**B** ACG											
B3	-3	5′-GTG ATA **B**GC		+8.0 [+1.5]	-2.5 [-1.0]	+18.0 [+1.0]	+28.5 [+4.0]	+22.0 [+0.5]	-	-	-	-	+10.5 [-1.0]
B4		3′-CAC **B**AT ACG											

[a] ΔT_m = change in T_m values relative to unmodified reference duplex **D1:D2** ($T_m \equiv 29.5$ °C); see Table 1 for experimental conditions; example of *DA* calculation: *DA* (**W1:W5**) = ΔT_m (**W1:W5**) − [ΔT_m (**W1:D2**) + ΔT_m (**D1:W5**)] = 25.0 °C - [7.0 °C + 15.5 °C] = +2.5 °C.

[b] Previously reported in reference 29.

Table 4

ΔT_m and *DA* values for DNA duplexes with interstrand zipper arrangements of pyrene-functionalized adenine monomers.[a]

			ΔT_m[*DA*]/°C			
ON	**Zipper**	**Duplex**	**B =**	**K**	**L**	**M**	**R**
B6 **B9**	+3	5′-GTG **B**TA TGC 3′-CAC TAT **B**CG	+12.0 [+1.5]	+13.0 [-10.0]	+16.0 [+4.0]	+10.0 [-1.0]
B6 **B8**	+1	5′-GTG **B**TA TGC 3′-CAC T**B**T ACG	-7.0 **[-18.5]**	-8.0 **[-30.5]**	-7.5 **[-21.0]**	-7.5 **[-20.5]**
B7 **B9**	+1	5′-GTG AT**B** TGC 3′-CAC TAT **B**CG	-5.0 **[-17.5]**	-7.0 **[-33.0]**	-8.0 **[-21.5]**	-7.0 **[-22.0]**
B7 **B8**	-1	5′-GTG AT**B** TGC 3′-CAC T**B**T ACG	+14.0 [+0.5]	+23.5 [-2.0]	+22.0 [+7.0]	+15.0 [-2.0]

[a] ΔT_m = change in T_m values relative to unmodified reference duplex **D1:D2** ($T_m \equiv 29.5$ °C); see Table 1 for experimental conditions.

Table 5

Efficiency of hairpin invasion of various Invaders at 100-fold probe excess.[a]

ON	Invader	% recognition
W2	5′-GTG A**W**A TGC	48 ± 11
W5	3′-CAC TA**W** ACG	
X2	5′-GTG A**X**A TGC	41 ± 12
X5	3′-CAC TA**X** ACG	
Y2	5′-GTG A**Y**A TGC	38 ± 2
Y5	3′-CAC TA**Y** ACG	
Q2	5′-GTG A**Q**A TGC	45 ± 14
Q5	3′-CAC TA**Q** ACG	
S2	5′-GTG A**S**A TGC	<5
S5	3′-CAC TA**S** ACG	
V2	5′-GTG A**V**A TGC	<5
V5	3′-CAC TA**V** ACG	
P2	5′-GTG A**P**A TGC	47 ± 3
P5	3′-CAC TA**P** ACG	
K6	5′-GTG **K**TA TGC	17 ± 3
K8	3′-CAC T**K**T ACG	
M6	5′-GTG **M**TA TGC	<5
M8	3′-CAC T**M**T ACG	
R6	5′-GTG **R**TA TGC	41 ± 4
R8	3′-CAC T**R**T ACG	

[a]Average of three independent measurements; “±” denotes standard deviation. For experimental conditions see Figure 6.